Formation Process of $LiSn_2(PO_4)_3$, a Monoclinically Distorted NASICON-Type Structure

Ana Martínez, José M. Rojo,* Juan E. Iglesias, Jesús Sanz, and Rosa M. Rojas

Instituto Ciencia de Materiales, CSIC, c/Serrano 115 dpdo, 28006 Madrid, Spain

Received April 5, 1994[⊗]

The formation of $LiSn_2(PO_4)_3$ from a stoichiometric mixture of Li_2CO_3, SnO_2, and $(NH_4)_2HPO_4$ heated in the temperature range 180–1200 °C has been followed by XRD, TG and NMR (^{119}Sn, ^{31}P, and ^{7}Li) techniques. Amorphous compounds and crystalline SnP_2O_7 have been identified as intermediate products. Two phases of $LiSn_2(PO_4)_3$ have been obtained: one coexists with SnO_2 and SnP_2O_7 while the other has been prepared as a single phase at 1200 °C. The spectroscopic and diffraction data agree with a rhombohedral $R\bar{3}c$ symmetry for the first phase and a monoclinic Cc symmetry for the second one.

Introduction

$LiSn_2(PO_4)_3$ belongs to the NASICON type compounds which are, in general, good conductors of alkali ions.[1–15] The framework is built up by $Sn_2(PO_4)_3$ units, which consist of two SnO_6 octahedra linked to each other by three PO_4 tetrahedra.[16–21] The Li^+ ions can be placed in two different sites: one, in an octahedral oxygen environment, at the intersection of three conduction channels (M1 site) and the other, at each bend of the conduction channels in a polyhedron of eight neighboring oxygens (M2 site). A middle position in between these two sites would be also available.

The lithium tin orthophosphate was firstly prepared[22] by heating stoichiometric amounts of Li_2CO_3, SnO_2, and $(NH_4)_2HPO_4$ at temperature close to 950 °C. Its X-ray powder diffraction pattern was indexed on the basis of the rhombohedral $R\bar{3}c$ space group with parameters a_R = 8.922(4) Å, α_R = 56°33(6)′ (a_H = 8.453, c_H = 22.407 Å). Moreover, two phases of $LiSn_2(PO_4)_3$ were prepared[23] by calcination of the same starting compounds at 950 and 1250 °C. Both phases were considered as NASICON type compounds, and their X-ray diffraction patterns were indexed on the basis of two rhombohedral lattices, which differ in cell volume by less than 1%. The main difference was the c/a ratio of 2.656 and 2.484 for the phases obtained at 950 and 1250 °C, respectively. However, for the sample prepared at 950 °C, an intense X-ray peak at 3.054 Å could not be indexed and the Raman spectrum showed more PO_4 vibration bands than those permitted by the rhombohedral symmetry.

In this paper the formation process of $LiSn_2(PO_4)_3$ has been followed by TG, XRD, and NMR (^{31}P, ^{119}Sn, and ^{7}Li) techniques. In particular, stoichiometric amounts of Li_2CO_3, SnO_2, and $(NH_4)_2HPO_4$ have been heated at different temperature in the 180–1200 °C range, and the intermediate products have been analyzed. A structural characterization of the two $LiSn_2(PO_4)_3$ phases has been also made.

Experimental Section

The reagents Li_2CO_3 (Fluka, >99.0%), SnO_2 (Aldrich, 99.9%), and $(NH_4)_2HPO_4$ (Fluka, >99%) were dried at 100 °C for 12 h. Stoichiometric amounts of these compounds were thoroughly mixed and calcined in air between 180 and 1200 °C, in a platinum crucible. Thermal treatments were accumulative. At each defined temperature the time spent was 6 h in the range 180–700 °C and 24 h above 700 °C. In all cases the mixture was ground before and after each treatment.

X-ray powder diffractograms were taken at room temperature by using a PW-1710 Philips diffractometer with Cu Kα radiation at a scanning rate of 1°/min, using a variable divergence slit such that the divergence was $2\theta/45$, given in degrees. For indexing purposes the patterns were recorded on a Siemens D501 diffractometer in the step scan mode with Cu Kα radiation, at a step value of 0.04°, measuring for 10 s at each step. The divergence slit was fixed at 0.3°, and a slit of 0.06° was placed in front of the receiving system formed by a graphite monochromator and a scintillation detector. Soller slits were used at both incident and diffracted beam collimat-

⊗ Abstract published in *Advance ACS Abstracts*, August 15, 1994.

(1) Goodenough, J. B.; Hong, H. Y-P.; Kafalas, J. A. *Mater. Res. Bull.* **1976**, *11*, 203.
(2) Shannon, R. D.; Taylor, B. E.; English, A. D.; Berzins, T. *Electrochim. Acta* **1977**, *22*, 783.
(3) Taylor, B. E.; English, A. D.; Berzins, T. *Mater. Res. Bull.* **1977**, *12*, 171.
(4) Petit, D.; Colomban, Ph.; Collin, G.; Boilot, J. P. *Mater. Res. Bull.* **1986**, *21*, 365.
(5) Sudreau, F.; Petit, D.; Boilot, J. P. *J. Solid State Chem.* **1989**, *83*, 78.
(6) Subramanian, M. A.; Subramanian, R.; Clearfield, A. *Solid State Ionics* **1986**, *18/19*, 562.
(7) Hamdoune, S.; Tranqui, D.; Schouler, E. J. L. *Solid State Ionics* **1986**, *18/19*, 587.
(8) Lin, Z.; Yu, H.; Li, S.; Tian, S. *Solid State Ionics* **1986**, *18/19*, 549.
(9) Casciola, M.; Costantino, U.; Merlini, L.; Krogh Andersen, I. G.; Krogh Andersen, E. *Solid State Ionics* **1988**, *26*, 229.
(10) Delmas, C.; Nadiri, A.; Soubeyroux, J. L. *Solid State Ionics* **1988**, *28–30*, 419.
(11) Chowdari, B. V. R.; Radhakrishnan, K. A.; Thomas, K. A.; Subba Rao, G. V. *Mater. Res. Bull.* **1989**, *24*, 221.
(12) Winand, J. M.; Depireux, J. *Europhys. Lett.* **1989**, *8*(5), 447.
(13) Aono, H.; Sugimoto, E.; Sadaoka, Y.; Imanaka, N.; Adachi, G. *J. Electrochem. Soc.* **1990**, *137*, 1023.
(14) Ado, K.; Saito, Y.; Asai, T.; Hiroyuki, K.; Nakamura, O. *Solid State Ionics* **1992**, *53–56*, 723.
(15) Nomura, K.; Ikeda, S.; Ito, K.; Einaga, H. *Solid State Ionics* **1993**, *61*, 293.
(16) Hagman, L.; Kierkegaard, P. *Acta Chem. Scand.* **1968**, *22*, 1822.
(17) Sljukic, M.; Matkovic, B.; Prodic, B.; Anderson, D. *Z. Kristallogr.* **1969**, *130*, 148.
(18) Hong, H. Y.-P. *Mater. Res. Bull.* **1976**, *1*, 173.
(19) McCarron, E. M.; Calabrese, J. C.; Subramanian, M. A. *Mater. Res. Bull.* **1987**, *22*, 1421.
(20) Mbandza, A.; Bordes, E.; Courtine, P.; El Jazouli, A.; Soubeyroux, J. L.; Le Flem, G.; Hagenmuller, P. *React. Solids* **1988**, *5*, 315.
(21) Alami, M.; Brochu, R.; Soubeyroux, J. L.; Gravereau, P.; Le Flem, G.; Hagenmuller, P. *J. Solid State Chem.* **1991**, *90*, 185.
(22) Perret, R.; Boudjada, A. *C. R. Acad. Sci. Paris* **1976**, *282*, C-245.
(23) Winand, J. M.; Rulmont, A.; Tarte, P. *J. Solid State Chem.* **1991**, *93*, 341.

0897-4756/94/2806-1790$04.50/0

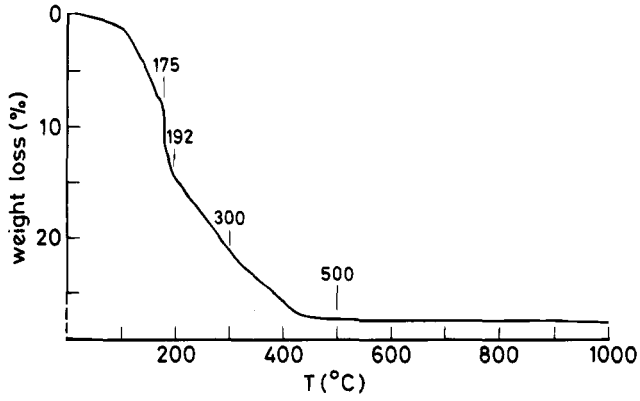

Figure 1. TG curve of the stoichiometric mixture of $(NH_4)_2HPO_4$, Li_2CO_3 and SnO_2 up to 1000 °C (still air, 2 °C/min heating rate).

ing systems, limiting the axial divergence to less than 5°. The peaks were fitted with $K\alpha_1-K\alpha_2$ doublets,[24] and the position of each peak was taken to be that of the $K\alpha_1$ component, for which a wavelength λ(Cu $K\alpha_1$ = 1.540 598 1 Å was assumed.

Thermogravimetric curves (TG) were obtained up to 1000 °C in still air, in a thermal analyzer Stanton STA 781 equipment at 2 °C/min heating rate. The sample was packed in a platinum holder and α-Al_2O_3 was used as reference.

^{31}P, ^{119}Sn, and ^{7}Li MAS NMR spectra were recorded at 161.96, 149.11, and 155.50 MHz, respectively, on a MSL 400 Bruker spectrometer. The samples were spun in the range 4.5–5.2 kHz. The spectra were taken after $\pi/2$ pulse irradiation (5 μs for ^{7}Li, and 4 μs for ^{119}Sn and ^{31}P). A time interval between successive scans of 30 s for the ^{31}P and ^{7}Li spectra and 60 s for the ^{119}Sn spectra was chosen. The number of scans was in the range 40–400. The ^{7}Li and ^{31}P chemical shift values are given relative to 1 M LiCl and 85% H_3PO_4 aqueous solutions, respectively. The reference for the ^{119}Sn spectra was a 5% solution of tetramethyltin in dichloromethane. All the spectra were recorded at room temperature.

Results

The thermogravimetric curve recorded on a mixture of stoichiometric amounts of SnO_2, $(NH_4)_2HPO_4$, and Li_2CO_3 is shown in Figure 1. A weight loss of 27.0% in the range 20–500 °C is observed. In addition, some changes of slope at 175, 192, and 300 °C are detected. Above 500 °C the reaction does not produce further weight loss.

The X-ray diffraction patterns corresponding to the mixture previously heated at some defined temperatures in the range 180–1200 °C are shown in Figure 2. The peaks of the different phases that do not overlap with other peaks have been labeled as follows: cassiterite SnO_2 (O), SnP_2O_7 (P), and the two $LiSn_2(PO_4)_3$ phases are referred to as I and II. The position of peaks corresponding to phase I and II agree with those reported by Winand et al.[23] for their samples prepared at 950 and 1250 °C, respectively. In this figure the X-ray patterns of the stoichiometric mixture heated at 180 and 300 °C show typical narrow peaks of SnO_2, as well as broad humps which are usually ascribed to amorphous compounds. In the range 375–700 °C, together with the SnO_2 peaks, reflections of SnP_2O_7 and the I and II phases are observed. The SnO_2 and SnP_2O_7 peaks disappear progressively on increasing the temperature. Above 700 °C, peak intensity of phase II

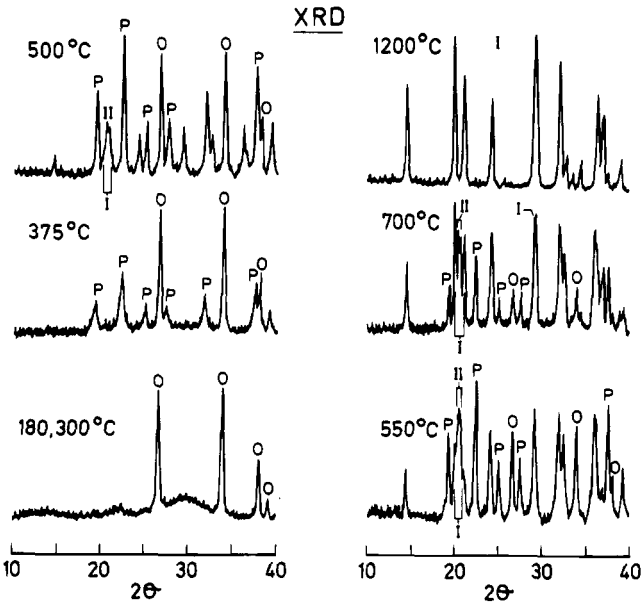

Figure 2. X-ray diffraction patterns recorded on the stoichiometric mixture heated at the indicated temperatures.

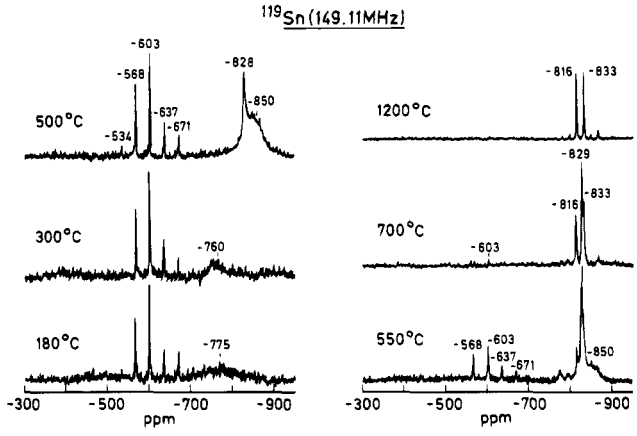

Figure 3. ^{119}Sn MAS NMR spectra of the stoichiometric mixture heated at the indicated temperatures.

decreases, and at 1200 °C only peaks of phase I are detected.

The ^{119}Sn MAS NNR spectra of the stoichiometric mixture heated at increasing temperatures are shown in Figure 3. At 180 and 300 °C the ^{119}Sn spectra are formed by a set of narrow lines at −534, −568, −603, −637, and −671 ppm, and a broad line at −775/−760 ppm. The central line of the set, placed at −603 ppm, defines the isotropic chemical shift value, while the others are sidebands of the central line. This set is similar to that reported[25] for SnO_2. The wide line at −775/−760 ppm should be associated with an amorphous compound, in agreement with the XRD data. In the range 375–500 °C this line disappears, and two new lines are observed: a wide one at about −850 ppm and another narrow one at −828 ppm. The line at −850 ppm, which is progressively eliminated above 500 °C, can be assigned to SnP_2O_7, according to the XRD data. Above 500 °C, the lines ascribed to SnO_2 disappear progressively and three narrow lines at −816, −829, and −833 ppm are clearly observed in the spectrum at 700

(24) Schreiner, W. N.; Jenkins, R. Norelco Reporter, APD Special Issue, 1983; p 66–69.

(25) Cossement, C.; Darville, J.; Gilles, J. M.; Nagy, J. B.; Fernandez, G.; Amoureux, J. P. *Magn. Reson. Chem.* **1992**, *30*, 263.

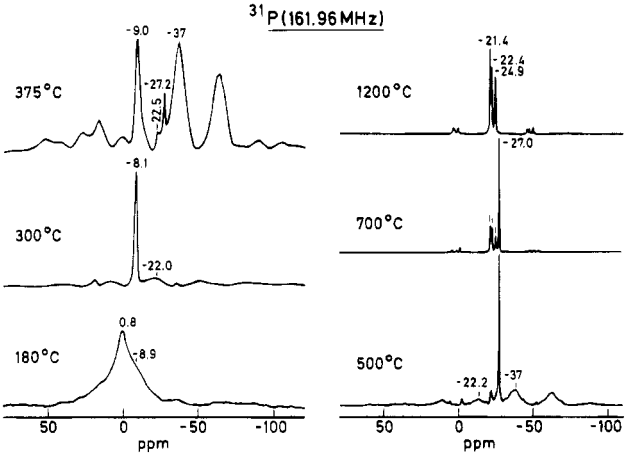

Figure 4. ^{31}P MAS NMR spectra of the stoichiometric mixture heated at the indicated temperatures.

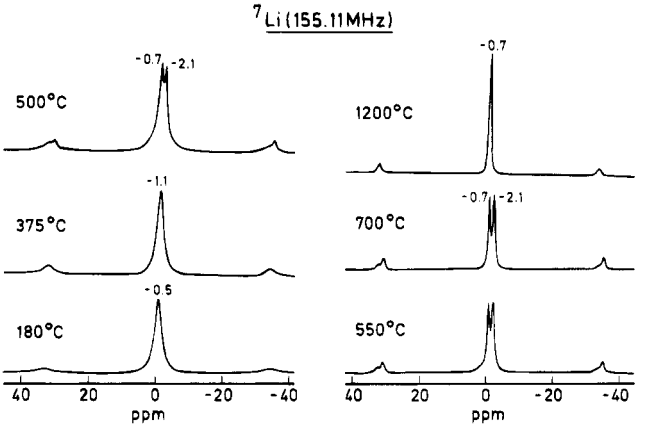

Figure 5. ^{7}Li MAS NMR spectra of the stoichiometric mixture heated at the indicated temperatures.

°C. On the basis of the fact that only phase I of $LiSn_2(PO_4)_3$ is obtained at 1200 °C, the lines at −816 and −833 ppm observed in the spectrum at this temperature are ascribed to that phase. The other line (−829 ppm) must be associated with phase II of that compound.

The ^{31}P MAS NMR spectra recorded on the stoichiometric mixture heated at increasing temperatures are shown in Figure 4. At 180 °C the spectrum consists of a broad line centered at 0.8 ppm and a shoulder at −8.9 ppm. When the mixture is heated at 300 °C the broad component is eliminated, the line at −8.1 ppm increases considerably, and a new broad component at about −22 ppm is observed. Moreover, two sets of sidebands separated at regular intervals from both lines are shown. At 375 °C, the spectrum shows, together with the line at −9.0 ppm, an intense line at −37 ppm and two narrow lines at −22.5 and −27.2 ppm. The other lines are sidebands. Above this temperature the lines at −9.0 and −37 ppm disappear progressively from the spectrum, the line at −27.2/−27.0 ppm remains up to 900 °C, and three lines at −21.4, −22.4, and −24.9 ppm are resolved. At 1200 °C the spectrum only shows the three latter lines. Taking into account that SnP_2O_7 is formed at about 375 °C and this compound is progressively eliminated above 500 °C, the complex line at −37 ppm can be assigned to tin pyrophosphate. In addition, its frequency is close to that reported[26] for SnP_2O_7 (−36 ppm). The three lines at −21.4, −22.4, and −24.9 ppm must be ascribed to phase I of $LiSn_2(PO_4)_3$ while that at −27.0 ppm is associated with phase II of that compound. The lines at 0.8, −8/−9, and −22 ppm observed at temperatures below 375 °C must correspond, according to the X-ray diffraction data, to some intermediate amorphous compounds formed in the first stages of the reaction.

The ^{7}Li MAS NMR spectra of the stoichiometric mixture heated at different temperatures are shown in Figure 5. In the range 180−375 °C a relatively wide line whose frequency changes from −0.5 to −1.1 ppm is observed. This line seems to be related to intermediate amorphous compounds already mentioned. Above 375 °C two lines are shown at −0.7 and −2.1 ppm, but some contribution of the former one must be present. In fact, the −0.7 and −2.1 ppm lines are better resolved in the range 500−700 °C. Above 700 °C, intensity of the line at −0.7 ppm increases while that of the line at −2.1 ppm diminishes. Both lines must be associated with the two $LiSn_2(PO_4)_3$ phases. Taking into account that at 1200 °C only phase I is obtained the line at −0.7 ppm is ascribed to this phase. The other line (−2.1 ppm) is associated with phase II.

Discussion

Formation Process. The stoichiometric reaction of $(NH_4)_2HPO_4$, SnO_2, and Li_2CO_3 to yield $LiSn_2(PO_4)_3$, according to

$$6(NH_4)_2HPO_4 + 4SnO_2 + Li_2CO_3 \rightarrow 2LiSn_2(PO_4)_3 + 12NH_3 + CO_2 + 9H_2O \quad (1)$$

must be accompanied by an overall weight loss of 27.9%. From the thermogravimetric curve in the range 20−500 °C (Figure 1) it is deduced a weight loss (27.0%), which agrees reasonably well with the theoretical prediction. In addition, several changes of slope at 175, 192, and 300 °C are observed suggesting that the reaction takes place through overlapping steps in which ammonia, carbon dioxide and water are removed. Above 500 °C no weight loss is appreciably detected in the thermogravimetric curve.

To get a better understanding of the reaction, the relative proportion of starting, intermediate, and final compounds, as deduced from intensity of the NMR lines ascribed to them, are plotted in Figure 6 as a function of temperature. For that the intensity of the central and its associated sidebands of the ^{119}Sn, ^{31}P, and ^{7}Li NMR spectra have been estimated.

Taking into account that pure $(NH_4)_2HPO_4$ decomposes at temperatures above 155 °C giving $NH_4H_2PO_4$:[27]

$$(NH_4)_2HPO_4 \rightarrow NH_4H_2PO_4 + NH_3 \quad (2)$$

such a reaction is expected. In fact, the broad line centered at 0.8 ppm in the ^{31}P NMR spectrum of the sample heated at 180 °C shows a frequency close to that

(26) Mudrakovskii, I. L.; Shmachkova, V. P.; Kotsarenko, N. S.; Mastikhin, V. M. *J. Phys. Chem. Solids* **1986**, *47*, 335.

(27) Bamford, C. H.; Tipper, C. F. H. *Comprehensive chemical kinetics*; Elsevier: Dordrecht, 1980; Vol. 22, Reactions in the Solid State.

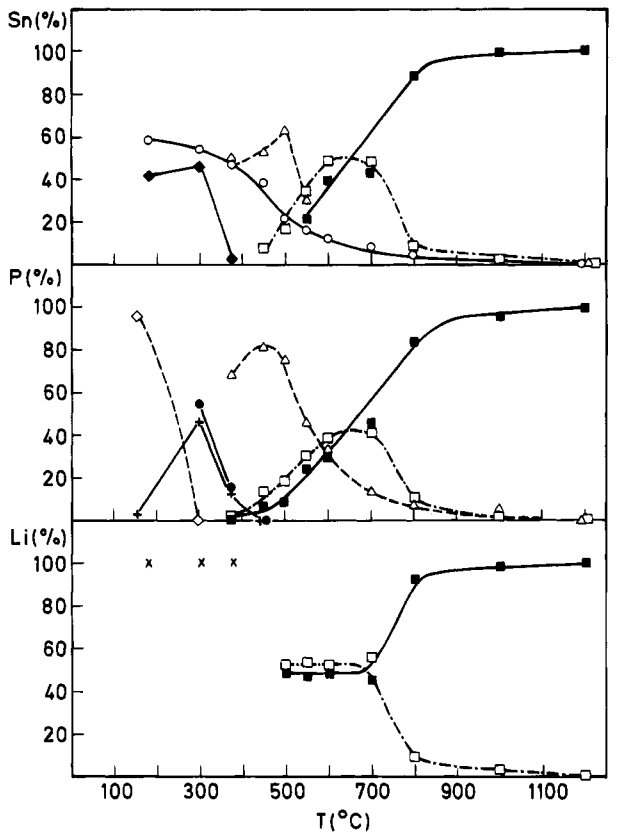

Figure 6. Relative intensity of the ^{119}Sn, ^{31}P, and ^{7}Li MAS NMR lines and their associated sidebands as a function of temperature. Crystalline compounds: SnO_2 (○), SnP_2O_7 (△), I $LiSn_2(PO_4)_3$ (■), II $LiSn_2(PO_4)_3$ (□). Amorphous compounds are denoted: ◆, ◇, +, ●, ×. The symbols are related as follow: ◆ to the ^{119}Sn line at −775/−760 ppm; ◇, +, and ● to the ^{31}P lines at 0.8, −8/−9, and −22 ppm, respectively; and × to the ^{7}Li line at −0.5/−1.1 ppm.

reported[28] for $NH_4H_2PO_4$ (0.9 ppm), although the absence of typical peaks of this compound in the X-ray diffractograms indicates that the atomic arrangement has no long-range order. The significant width of the line suggests the presence of components associated with other amorphous phosphates. In fact, at this temperature Li_2CO_3 and a portion of SnO_2 (42%) have also reacted as deduced from the broad lines at −760 and −0.5 ppm in the ^{119}Sn and ^{7}Li NMR spectra, respectively.

When the mixture is heated at 300 °C, $NH_4H_2PO_4$ is eliminated and only an additional small amount (4%) of SnO_2 has reacted (Figure 6). At this temperature the ^{119}Sn spectrum is similar to that found at 180 °C. However, several changes are observed in the ^{31}P spectrum. Thus, the line at 0.8 ppm disappears and two lines are clearly detected: one at −8.1 ppm and another wider line at −22 ppm. The line at −8/−9 ppm should be ascribed to an intermediate compound and that at −22 ppm, whose frequency is close to those of phases I and II, would be associated with an amorphous precursor of $LiSn_2(PO_4)_3$. The relative intensities of those lines are 45 and 55%, respectively.

In the range 300−450 °C the amorphous compounds are progressively transformed into SnP_2O_7 and the two $LiSn_2(PO_4)_3$ phases, as deduced from intensity of the ^{119}Sn and ^{31}P lines ascribed to those products (Figure 6). At 450−500 °C the amount of SnP_2O_7 attains its highest value. The ^{7}Li NMR spectra of the mixture heated at these temperatures (400−500 °C) shows two new lines at −0.7 and −2.1 ppm. They are better resolved when the mixture is heated at higher temperature, suggesting some contribution of the unresolved component (−0.5/−1.1 ppm) corresponding to lithium in amorphous intermediates.

Above 500 °C tin pyrophosphate, tin dioxide, and the amorphous lithium "reservoir" are transformed into $LiSn_2(PO_4)_3$. In fact, a progressive decrease in intensity of the ^{119}Sn and ^{31}P lines associated with the two former products is observed (Figure 6). The amount of phases I and II of $LiSn_2(PO_4)_3$ increases between 500 and 700 °C, and phase I is developed at the expense of phase II in the range 700−1200 °C. The last observation goes parallel with the intensity variation deduced from the ^{7}Li NMR spectra. Thus, intensity of the −0.7 ppm line increases, while that of the −2.1 ppm line decreases simultaneously.

Characterization of the Two $LiSn_2(PO_4)_3$ Phases. From the above results it can be seen that in the studied temperature range, phase II always coexists with other compounds such as SnO_2 and SnP_2O_7. However, it has been obtained by Winand et al.[23] as a single phase and its X-ray diffraction pattern indexed on the basis of a rhombohedral lattice, whose parameters expressed in terms of an hexagonal cell were $a = 8.650(1)$ and $c = 21.487(5)$ Å; the assigned Miller indices are consistent with the space group $R\bar{3}c$. Our spectroscopic data agrees with this symmetry. Indeed, the ^{31}P and ^{119}Sn NMR spectra of phase II consist of one line at −27.0 and −829 ppm, respectively, indicating the existence of only one independent crystallographic site for phosphorus and another one for tin.

On the other hand, phase I which has been obtained by us as a single phase shows a X-ray diffractogram similar to that previously reported.[23] A trial using our data and an automatic indexing routine (TREOR) has led to hexagonal parameters $a = 8.459(2)$, $c = 22.440(9)$ Å, which are in agreement with those reported by Winand et al.[23] ($a = 8.444(2)$ and $c = 22.424(8)$ Å), and by Perret and Boujdada[22] ($a = 8.453$, $c = 22.407$ Å). However, several peaks remain unindexed, the most prominent one being that observed at 3.049 Å, and others at 1.915 and 1.902 Å. In addition, it should be remarked that the indexing published,[23] which we reproduce for comparison with ours in Table 1, presents the problem that at least two peaks have indices in conflict with the space group $R\bar{3}c$, those indexed as (303) and (01 11). The space group $R\bar{3}c$ is the usual one in the rhombohedral structures of the NASICON type materials.[4,16-21] The need to index all the X-ray peaks, together with the presence of more ^{31}P and ^{119}Sn NMR lines than permitted by the space group $R\bar{3}c$ led us to consider a lower symmetry. In analogy with the monoclinic distortion which has been reported[3,4,5,29,30] for $LiZr_2(PO_4)_3$ we have been able to index the pattern of $LiSn_2(PO_4)_3$ on the basis of a monoclinic cell with parameters $a = 14.6656(7)$, $b = 8.4052(4)$, $c = 8.8933(4)$ Å, $\beta = 122.986(4)°$; the estimated standard deviations

(28) Turner, G. L.; Smith, K. A.; Kirkpatrick, R. J.; Oldfield, E. *J. Magn. Reson.* **1986**, *70*, 408.

(29) Alamo, J.; Rodrigo, J. L. *Solid State Ionics* **1989**, *32/33*, 70.

(30) Sanz, J.; Rojo, J. M.; Jimenez, R.; Iglesias, J. E.; Alamo, J. *Solid State Ionics* **1993**, *62*, 287.

Table 1. Powder Pattern of Phase I, Monoclinic $LiSn_2(PO_4)_3$ (Rhombohedral Indexing after Winand et al.,[23] Doubtful Indexes Marked*)

h k l monoclinic	$2\theta_{calc}$	$2\theta_{obs}$	d_{calc}	d_{obs}	*I*	*h k l* rhombohedral (hexagonal axes)
2 0 0	14.39		6.151			
		14.48		6.112	30	0 1 2
1 1 −1	14.51		6.101			
1 1 1	19.96		4.446			
		19.99		4.438	100	1 0 4
2 0 −2	20.01		4.435			
3 1 −1	21.01		4.226			
		21.07		4.213	50	1 1 0
0 2 0	21.12		4.203			
3 1 0	24.13		3.685			
3 1 −2	24.24	24.24	3.669	3.669	35	1 1 3
0 2 1	24.29		3.662			
4 0 0	29.01	29.03	3.075	3.073	35	0 2 4
2 2 −2	29.25	29.27	3.050	3.049	55	
3 1 1	31.89	31.92	2.8039	2.8014	28	
0 2 2	32.06		2.7896			1 1 6
		32.07		2.7888	37	
3 1 −3	32.07		2.7889			
5 1 −2	32.58		2.7464			
		32.60		2.7445	4	2 1 1
4 2 −1	32.61		2.7435			
1 3 0	32.76	32.76	2.7318	2.7316	2	
5 1 −1	33.26	33.27	2.6919	2.6908	1	
1 3 −1	33.52	33.48	2.6716	2.6744	1	
2 0 2	34.21		2.6191			
		34.33		2.6101	4	0 1 8
1 1 −3	34.34		2.6091			
4 2 0	36.16	36.21	2.4818	2.4788	12	
5 1 −3	36.25		2.4761			2 1 4
		36.34		2.4703	20	
1 3 1	36.34		2.4704			
6 0 −2	36.74	36.77	2.4442	2.4423	11	
3 3 −1	36.95	36.96	2.4308	2.4302	17	3 0 0
2 2 −3	37.44	37.49	2.4001	2.3970	1	
3 3 0	38.90		2.3133			
		38.92		2.3122	5	3 0 3
3 3 −2	38.97		2.3091			
2 2 2	40.55	40.56	2.2228	2.2224	2	
4 0 −4	40.66	40.67	2.2173	2.2166	3	2 0 8
1 1 3	42.17		2.1413			
		42.23		2.1383	7	1 0 10
2 0 −4	42.26		2.1367			
6 2 −2	42.76	42.78	2.1129	2.1121	5	2 2 0
0 4 0	43.01	43.02	2.1013	2.1008	3	
5 1 −4	43.32	43.34	2.0871	2.0861	2	
6 0 0	44.14	44.14	2.0503	2.0502	3	
3 3 −3	44.52	44.49	2.0336	2.0348	7	3 0 6
7 1 −3	45.35		1.9980			
5 3 −1	45.42	45.46	1.9951	1.9936	3	
2 4 0	45.58		1.9885			
5 1 1	45.94	45.95	1.9739	1.9735	1	4 2 8*
4 2 −4	46.26		1.9611			
		46.30		1.9594	7	0 1 11
1 3 −3	46.27		1.9606			
7 1 −1	47.45		1.9144			
		47.45		1.9145	10	0 2 10*
4 0 2	47.42		1.9155			
2 2 −4	47.71		1.9047			
5 3 −3	47.77	47.79	1.9023	1.9017	13	1 3 4*
2 4 −2	47.86		1.8989			
6 2 0	49.42	49.43	1.8427	1.8424	5	
6 2 −4	49.67		1.8341			
		49.73		1.8319	9	2 2 6*
0 4 2	49.76		1.8309			
8 0 −2	50.35	50.34	1.8109	1.8112	<1	
4 4 −2	50.72	50.70	1.7985	1.7991	1	
4 2 2	52.46	52.46	1.7430	1.7429	7	
1 3 3	52.64		1.7373			4 0 4
		52.67		1.7364	12	2 1 10
5 1 −5	52.70		1.7356			
7 1 0	53.21	53.22	1.7202	1.7197	<1	
5 3 −4	53.62		1.7080			
		53.66		1.7067	<1	
2 4 −3	53.67		1.7064			
5 3 1	55.87	55.87	1.6442	1.6443	2	
7 1 −5	56.04		1.6398			
		56.06		1.6392	3	
2 4 2	56.07		1.6390			
7 3 −1	57.19		1.6093			
		57.26		1.6076	6	
8 2 −4	57.30		1.6067			
1 5 1	57.53		1.6006			
		57.56		1.6000	7	
9 1 −3	57.57		1.5997			
6 4 −2	57.82		1.5934			
		57.93		1.5906	6	
3 5 −1	57.97		1.5897			
1 1 −5	59.16	59.16	1.5604	1.5605	2	
7 1 1	61.38	61.37	1.5093	1.5094	4	
5 3 −5	61.86		1.4987			
		61.87		1.4984	7	
2 4 −4	61.88		1.4982			

quoted have been obtained from a Rietveld refinement now in progress. The indexed pattern is shown in Table 1. It can be seen that the intense peak at 3.049 Å is now indexed as $(22\bar{2})_{mon}$; this peak and the $(400)_{mon}$ come from splitting of the $(024)_{rh}$. All peaks reported[23] as of doubtful indexing (they appear marked with asterisks in Table 1) are adequately accounted for. Further support to this indexing is provided by the observed splitting of several ideal rhombohedral reflections:

(i) $(116)_{rh}$ splits into $(311)_{mon}$, $(022)_{mon}$, and $(31\bar{3})_{mon}$, with spacings calculated at 2.8039, 2.7896, and 2.7889 Å, of which only two resolved peaks are seen at 2.8014 and 2.7888 Å.

(ii) $(214)_{rh}$ splits into $(420)_{mon}$, $(51\bar{3})_{mon}$, and $(131)_{mon}$, predicted at 2.4818, 2.4761, and 2.4704 Å; we observe two very close peaks at 2.4788 and 2.4703 Å.

(iii) $(300)_{rh}$ splits into $(60\bar{2})_{mon}$ and $2\times(33\bar{1})_{mon}$, which we observe at 2.4423 and 2.4302 Å, in agreement with their predicted values of 2.4442 and 2.4308 Å.

Other splittings can be deduced from an attentive study of the data in Table 1.

Our indexing is consistent with a monoclinic C lattice. The X-ray data show systematic absence of reflections *h0l* with *l* odd, so the possible space groups are *C2/c* or *Cc*. For space group assignment the spectroscopic features must be considered. Thus, the ^{31}P NMR spectrum shows three lines with the same intensity at −21.4, −22.4, and −24.9 ppm (Figure 4), while two equal lines at −816 and −833 ppm are observed in the ^{119}Sn NMR spectrum (Figure 3). The presence of three crystallographically independent phosphorus and two tin sites supports the space group *Cc*.

Finally, two lines at −0.7 and −2.1 ppm are observed in the ^{7}Li NMR spectra of phases I and II, respectively. On the basis that in other rhombohedral $LiM_2(PO_4)_3$ (M = Zr, Ge) samples lithium occupies preferentially the M1 site,[4,21] the line at −2.1 ppm observed only in the spectrum of phase II is assigned to lithium in that site. Taking into account that the NASICON framework shows two very different environments for alkali ions in the M1 and M2 sites, the other line (−0.7 ppm) would be ascribed to lithium in the M2 environment. In the monoclinic phase I, the *Cc* symmetry should induce a

differentiation of the M2 sites into three types; however, only one line at −0.7 ppm is observed suggesting that the new M2 environments are similar. The position of the two ^{7}Li lines are close to that found for $LiZr_2(PO_4)_3$. In this case, the observed lines at −0.8 and −1.4 ppm in the ^{7}Li NMR spectrum have been assigned[30] to lithium placed in the M2 and M1 environments, respectively.

Conclusions

Intermediate amorphous compounds are formed in the first stages of the reaction (180−300 °C). Between 300 and 450 °C they are partially transformed into SnP_2O_7, and above 450 °C two phases of $LiSn_2(PO_4)_3$ are obtained. One (phase II) coexists with SnO_2 and SnP_2O_7 in the range 450−1100 °C, the other (phase I) has been prepared as a single phase at 1200 °C.

Phase II shows one site for phosphorus and another one for tin, which is in agreement with the rhombohedral $R\bar{3}c$ symmetry of the NASICON framework. In phase I we have detected three phosphorous and two tin sites, which supports a monoclinic *Cc* symmetry. By using a monoclinic cell of parameters $a = 14.6656(7)$, $b = 8.4052(4)$, $c = 8.8933(4)$ Å, $\beta = 122.986(4)°$, the X-ray powder diffraction pattern of phase I has been fully indexed. Two lithium environments related to M1 and M2 sites of the NASICON framework have been also identified.

Acknowledgment. Financial support by CICYT of Spain (Project MAT 92-0202) is gratefully acknowledged.